Supporting Information

Title: 3D printing of biomimetic vasculature for tissue regeneration

Author(s), and Corresponding Author(s)*: Dong Lei,[a,b] Yang Yang,[c] Zenghe Liu,[a,b] Binqian Yang,[b] Wenhui Gong,[d] Shuo Chen,[b] Shaofei Wang,[b] Lijie Sun,[b] Benyan Song,[b] Huixia Xuan,[b] Xiumei Mo,[a] Binbin Sun,[a] Sen Li,[c] Qi Yang,[c] Shixing Huang,[c] Shiyan Chen,[b] Yiding Ma,[b] Wenguang Liu,[e] Chuanglong He,[a] Bo Zhu,[f] Eric M. Jeffries,[g] Feng-Ling Qing,[a] Xiaofeng Ye,[c]* Qiang Zhao[c]* and Zhengwei You[a,b]*

[a] State Key Laboratory for Modification of Chemical Fibers and Polymer Materials, College of Chemistry, Chemical Engineering and Biotechnology, Donghua University, Shanghai , 201620, China

E-mail: zyou@dhu.edu.cn.

[b] State Key Laboratory for Modification of Chemical Fibers and Polymer Materials, International Joint Laboratory for Advanced Fiber and Low-dimension Materials, College of Materials Science and Engineering, Donghua University, Shanghai, 201620, China

[c] Department of Cardiac Surgery, Ruijin Hospital, Shanghai Jiaotong University School of Medicine, Shanghai, 200025, China

E-mail: zq11607@rjh.com.cn, xiaofengye@hotmail.com.

[d] Department of Cardiovascular Surgery, The first Affiliated Hospital of Anhui Medical University, Hefei, 230022, China

[e] School of Materials Science and Engineering, Tianjin Key Laboratory of Composite and Functional Materials, Tianjin University, Tianjin, 300072, China.

[f] School of Materials Science & Engineering, Shanghai University, Shanghai, 200444, China

[g] 6120 Fillmore Place, Apt 2 West, New York, NJ 07093, USA

Experimental method

Fabrication and characterization of sacrificial caramel-based template

The commercially available white granulated sugar (sucrose ≥ 99.5%) was used as raw materials of 3D printing. Sucrose powder was preheated to 150 °C for 30 minutes in the extruder of rapid prototyping system (HTS-400; Fochif Mechatronics Technology, China) to be caramelized moderately. Then the temperature was decreased to 135 °C for 10 minutes. The melted sucrose was squeezed out by extrusion ram with a nozzle temperature of 130 °C and directly deposited on an acrylic plate to form three-dimensional sacrificial caramel template according to the expected pattern path. The length and width of 3D sacrificial templates were both 20 mm. The center-to-center distance between filaments was 1.2 mm or 1.5 mm or 1.8 mm with 0°/90° or -45°/45° lay-down patterns between two successive layers. The height of every layer was 0.5 mm. Extrusion rate was 0.001 mm/s. Extruder internal diameter was 20 mm. Nozzle size was 21G. In order to obtain templates with better morphology, different moving rates of extrusion nozzle were investigated (0.5 mm/s, 0.75 mm/s, 1.0 mm/s, 1.2 mm/s, 1.4 mm/s, 1.6 mm/s, 1.8 mm/s, 2.0 mm/s, 2.5 mm/s, 3.0 mm/s, 4.0 mm/s). 3D printed templates were imaged using optical microscopy (Eclipse E400 POL, Nikon, Japan), and the diameters of filaments were measured by the accessary software. Dendritic templates were printed by 3D-Bioplotter® (Manufacturer Series, EnvisionTEC, Germany). For compression testing, crisscrossed templates with 15 layers were tested by a universal testing system (INSTRON-5969, Instron, USA) with a 100 N sensor. The samples were compressed to failure at a speed of 2 mm/min.

Fabrication and characterization of PHMs

Polycaprolactone (HMW-PCL, M_n 80,000 g/mol) was solubilized in hexafluoroisopropanol (HFIP, 98%) or tetrahydrofuran (THF, 99%) or dichloromethane (DCM, 99%) with magnetic stirring for 6 h to a clear solution. In order to get the scaffold with certain porosity and surface morphology, different concentrations (3% w/v, 4% w/v, 5% w/v) were used. Low molecular weight PCL (LMW-PCL, M_n 50,000 g/mol) PHMs was fabricated using HFIP as solvent in concentration of (4%). The caramel-based template was immersed in PCL solution for 1 min, and the solvent was allowed to evaporate for 30 min at an ambient temperature. Then the template with PCL coating was immersed in distilled water for 3 hours to eliminate caramel and residual solvent. The water was changed every hour. Then PCL scaffold was freeze-dried in vacuum. To illustrate the rapid removal process of templates, a few drops of distilled water were added to one side of the PCL polymer coated template. The whole process was monitored by a microscope (Eclipse E400 POL, Nikon, Tokyo, Japan). To illustrate the multi-level structure of the PHMs, scaffolds were imaged by SEM (JSM-5600LV, Jeol, Ltd., Tokyo, Japan). SEM image data were analyzed using the NIH ImageJ version 1.51. The mechanical properties of PHMs were evaluated by tensile test and compression test using the universal testing machine with a 100 N sensor (MTS Echo, Exceed 40, America) , which was equipped with the software TestSuite TW. PHMs were cut into strips and stretched along the channels direction in simple tensile tests and cyclic tensile tests with a maximum strain of 20% for 10 cycles at a rate of 10 mm min^{-1}. The moduli were calculated by taking the initial slope of the stress-strain curve. In the cyclic compression test, the specimens were compressed to a large strain of 40% for 10 cycles at a rate of 2 mm min^{-1}.

In order to verify the perfusability of the PHMs, glass tubes as inlet and outlet were installed in the HMW-PHMs with a syringe pump to assemble a microfluidic device. The joint was sealed with 10% (w/v) PCL/HFIP solution to prevent leakage. The red dye solution (reactive brilliant red, K-2BP, Tianjin, China) was pumped into PHMs. The process was recorded by the microscope.

Fabrication and characterization of elastic PCL-PU and PGSU PHMs

PCL-PU was synthesized in two steps as previously report[1]. In the first step, isocyanate terminated pre-polymers were synthesized by reacting PCL polyol (M_n 2,000 g/mol, Sigma; 2.5 mmol, 5g) with excessive hexamethylene diisocyanate (HDI, 99%, Aladdin; 15 mmol, 2.52g) at 80 ^oC for 3 h under a dry nitrogen atmosphere. Then, the reaction temperature was lowered to 60 ^oC. In the second step, dibutyltin dilaurate (97.5%, J&K; 0.5% w/w) was added to the pre-polymers as a catalyst. The chain extender 1,4-butanediol (99%, TCI; 12.5 mmol, 1.125g) was dissolved in N,N-dimethylformamide (DMF, 99%) was added dropwise to the reaction mixture. The reaction temperature was slowly raised to 80 ^oC and kept at this temperature for 3 hours with stirring. The subsequent molar ratio of HDI/ 1,4-butanediol /PCL was 6/5/1. The molecular structure of products was characterized by ^1H nuclear magnetic resonance (NMR, Bruker Avance 600 NMR). The caramel templates were immersed in the PCL-PU/HFIP solution (4% w/v) for 1 min, and the solvent was allowed to evaporate for 30 min at ambient temperature. Then the templates with PCL-PU coating were immersed in distilled water for 3 hours to eliminate caramel and residual solvent, and the water was changed every hour.

PGSU was synthesized as previously report[2]. PGS pre-polymer was synthesized through the polycondensation of equimolar amounts of glycerol (analytical grade, 99%, TCI) and sebacic acid (analytical grade, 99%, TCI) at 120 ^oC and under nitrogen atmosphere for 8 hours. The pressure was reduced using an in-house vacuum line and the reaction followed for 16 hours, yielding a pale-yellow viscous pre-polymer. The PGS pre-polymer was solubilized in HFIP (10% w/v) in the presence of the catalyst stannous 2-ethyl-hexanoate (Tin (II), Sigma; 0.05% w/v). HDI was added dropwise to the PGS pre-polymer solution (molar ratio of glycerol:HDI = 1:1). The caramel templates were immersed in the solution for 1 min, and the solvent was allowed to evaporate for 30 min at ambient temperature. The coated caramel-based templates were crosslinked at 60 ^oC and under nitrogen atmosphere for 24 hours. Then the templates with poly (glycerol sebacate urethane) (PGSU) coating were immersed in distilled water for 3 hours to eliminate caramel and residual solvent, and the water was changed every hour. Both of PCL-PU PHMs and PGSU PHMs were freeze-dried in vacuum. ATR-FTIR spectroscopy of the PCL-PU and PGSU PHMs was recorded by a Thermo Nicolet IR iS 10 spectrometer.

PCL-PU and PGSU elastic scaffolds were imaged by SEM. SEM images data were analyzed using the NIH ImageJ version 1.51. The mechanical properties of PCL-PU and PGSU PHMs were evaluated by tensile and compression tests. PHMs were cut into strips and stretched along the channels direction in ultimate tensile strength test and 10 cycles tensile fatigue test with strain of 20% at a rate of 10 mm min^{-1}. The modulus was calculated by taking the initial slope of the stress-strain curve. In the cyclic compression test, the specimens were compressed to a strain of 40% in loading-unloading for 10 cycles at a rate of 2 mm min^{-1}. The dynamic tensile strength restoration was measured at a strain of 10% from 2nd to 10th cycles compared to 1st cycle.

Fabrication and characterization of composite scaffolds with built-in PHMs

Porous scaffold with build-in PHMs was prepared by combining aforementioned HMW-PHMs fabrication process with modified salt fusion method. Briefly, NaCl salt particles with a size range of 38−76 μm were put into the interstitial space between filaments of caramel-based template. The two-component mold was transferred to and kept in a humidified incubator at 37 °C for 5 min. The caramel-based template and salt particles were slightly fused and integrated in a vacuum oven at 37 °C under 1 Torr. The two-component integrated mold was immersed into an HFIP solution of HMW-PCL (4%, w/v) for 3 min. The HFIP was allowed to evaporate completely for 30 min. The resultant PCL impregnated two-component mold was soaked in deionized water for 3 hours to eliminate caramel, salt particles and residual solvent. The water was changed every hour. The porous scaffolds with build-in interconnected channeled network were freeze-dried in vacuum and were imaged by SEM in top view and section view.

PHMs composite scaffolds with nanofibers were prepared by electrospining. The above HMW-PCL PHMs was used as a receiver. And a HMW-PCL solution (12.5 %, w/v) in HFIP was pumped out via a 21-gauge needle at a flow rate of 0.8 ml/h with a high positive voltage of 10 kV applied. Electrospun nanofibers were deposited on the PHMs and imaged by SEM under different magnification in top view and section view.

Bacterial cellulose composite scaffold with build-in PHMs was prepared by using HMW-PCL PHMs as a growth template for microorganism fermentation. Gluconacetobacter xylinus strain (1.1812), purchased from Institute of Microbiology, Chinese Academy of Science, was incubated statically with PHMs as a template in basal culture medium (glucose 5 wt%, yeast extract 0.5 wt%, bacto-peptone 0.5 wt%, disodium phosphate 0.2 wt%, monopotassium phosphate 0.1 wt% and citric acid 0.1 wt%, the pH was adjusted to 5.0 with NaOH) at 30 ^{o}C for five days. Then the synthesized cellulose were washed in ethylalcohol for 12 hours in order to remove the remaining culture medium and microorganism, and then repeatedly rinsed with pure water until filtrate became neutral. The bacterial cellulose composite scaffolds were freeze-dried in vacuum and were imaged by SEM in top view and section view.

Hydrogel composite scaffold with build-in HMW-PCL PHMs was prepared by encapsulating PHMs with alginate hydrogel. Sodium alginate (AGS, low viscosity, cell culture tested, Sigma, USA) and calcium chloride dehydrate ($CaCl_2$, suitable for cell culture, Sigma, USA) were respectively dissolved in distilled water with stirring to obtain aqueous solution (AGS, 3%, w/v; $CaCl_2$ 10%, w/v). PHMs were immersed in AGS solution on a watchglass. $CaCl_2$ aqueous solution was sprayed on the AGS solution encapsulated PHMs to form the gel of sodium alginate with divalent cation as Ca^{2+}. In addition, we further prepared a microvasculature system by encapsulating PHMs with inlet and outlet as described previously. The red dye solution was pumped into PHMs. The process was recorded by the microscope.

3D cell culture of cardiomyocytes

The H9c2 cells line was brought from Tipical Culture Collection cell bank of Chinese Academy of Sciences Committee and cultured in high glucose (4,500 mg/l) Dulbecco's modified Eagle's medium (DMEM) supplemented with 10% fetal bovine serum (FBS) and 1% penicillin-streptomycin (Gibco-BRL Inc., Grand Island, NY, USA) at 37 °C in a 95% air/5% CO_2 incubator. H9c2 cells were seeded at a density of 10,000 cells/cm^2. Seeding was performed in a 6-well flat-bottom plate. After 48 hours, the culture medium and unattached cells

were aspirated and fresh medium was added. At 2-day intervals, the medium together with unattached cells was removed and fresh medium was added.

The PHMs were divided into three groups: monolithic alginate cell-laden hydrogels, cell-laden hydrogels group with built-in HMW-PCL PHMs, and typical 3D-printed solid PCL scaffolds within cell-laden gels. Prior to cell seeding, PHMs, typical 3D-printed solid PCL scaffolds and spray bottle were sterilized with ethylene oxide, and subsequently washed with phosphate-buffered saline (PBS, 1X, Sterile). Centrifuge tubes and scissors were sterilized with high temperature and high pressure. AGS/PBS solution (4%, w/v), $CaCl_2$ solution (50 mg/ml) were sterilized under ultraviolet radiation for 24 h. AGS and $CaCl_2$ solutions were filtered through a sterile filter (Millipore, 0.22 μm) in a centrifuge tube for further sterilization; $CaCl_2$ solution transferred to a sterile spray bottle. When H9c2 myocardial cells amplified to 4 large Petri dish covered (1~2 $\times 10^6$ per plate), digested, centrifuged and separated to cell concentration of 4×10^6 ml^{-1} (1 ml). 3 ml AGS solution was solubilized in 1 ml cell suspension with wind mixing, then static and removed bubble to form AGS&cell mixture (3%, w/v) AGS (cell concentration was 1×10^6 ml^{-1}). $CaCl_2$ solution were sprayed on leveled mixture and then remained still for 10 min to fabric the crosslinked monolithic cell-laden hydrogels. Dispensing the mixture around a carbohydrate-glass lattice hollow PHMs and typical 3D-printed solid scaffolds, then carefully crosslinked with atomized $CaCl_2$ solution for 10 min. Three groups were cultured in aforementioned medium for 5 days. The samples were stained with a Live-Dead Cell Staining Kit (KGAF001, Keygen, China) and observed under inverted fluorescent contrast phase microscope (Eclipse Ti-E, Nikon, Japan) 1 hour after cell seeding. After 5 days culture, samples were stained with a Live-Dead Cell Staining Kit and observed by confocal laser scanning microscope (LSM710, Zeiss, Germany). For CCK-8 assay, a CCK-8 solution (KGA317, Keygen, China) was added to each of samples t 1 day, 3 days and 5 days. After cultured 3.5 h in a fully humidified incubator (37 ^oC, 5% CO_2), the absorbance at a wavelength of 450 nm was measured by a SynergyMX plate reader (Biotek, Winooski, VT).

***In vivo* tissue regeneration, angiogenisis and myocardial application of PHMs**

All animals were utilized following the Laboratory Animal Care Facility of Shanghai Medical College at Fudan University in accordance with the Guide for the Care and Use of Laboratory Animals (National Institutes of Health, Publication No. 85-23, Revised). Eighteen Standard Sprague-Dawley rats (SD, male, 180 g) from an in-house breed of the local animal care facility were used for *in vivo* model. All rats were anesthesia by 2% pentobarbital via abdominal injection. For subcutaneous implantation, two subcutaneous pouches (1 cm long) were created via dissecting the posterior dorsum skin of 9 rats. Disk-shaped HMW-PCL PHMs and typical printed scaffold (6 mm diameter) were placed into each pouch and the skin incision was sutured with 3/0 Mersilk (Ethicon, UK). Three rats from each subcutaneous implantation group were sacrificed on specialized time point (1, 7 and 14 days post-implantation). For epicardial implantation, 6 rats were anesthetized followed by intubation and respiratory support provided by a rodent ventilator (683 Ventilator, Harvard Apparatus, Holliston, MA). The heart was exposed through a left thoracotomy and the disk-shaped HMW-PCL PHMs and typical printed scaffold (6 mm diameter) were affixed on the left ventricular epicardium using 5-0 polypropylene (Ethicon, UK). Rats were sacrificed 14 days post-implantation. For application in myocardial infarction model, 12 rats were devided into the following three groups randomly: myocardial infarction control (n = 4), healthy control (n = 4), typical printed scaffold (n = 4) and HMW-PCL PHMs (n = 4). Ligation of the left

anterior descending coronary artery with 5-0 polypropylene suture was performed through a left thoracotomy. Subsequently, typical printed scaffolds and PHMs were implanted on the anterior infarcted myocardium with 5-0 polypropylene suture. Rats were sacrificed 4 weeks post-implantation. To perform histological evaluation, specimens were extracted. and fixed in 10% formalin buffer, dehydrated in graded ethanol and xylene, and then embedded in paraffin. In term of the subcutaneous tissues, a series of 8 μm-thick sections were cut. The heart tissues were sectioned at 8 μm in the LV transverse direction in the middle of the implants. Subsequently, all specimens were stained with hematoxylin and eosin (H&E) according to the standard procedure. Viable myocardium area and fibrosis area were measured using ImageJ software (ImageJ 1.46, National Institute of Mental Health, Bethesda, MD). Immunofluorescence analysis was performed to investigate the vascular formation and inflammatory reaction of the heart tissues. Sections were fixed in 4% paraformaldehyde and blocked with 2% goat serum for 1 h at room temperature, immunolabeled with primary antibody against von Willebrand factor (vWF) (ab6994; 1:100, Abcam) , and primary antibody against CD68 (ab125212; 1:100, Abcam) followed by goat anti-rabbit secondary antibody Alexa 488 (A-1108; 1:200, Thermo Fisher Scientific). Nuclear staining was performed by incubating sections with Vecta shield mounting medium containing 40,6-diamidino-2-phenylindole (DAPI, H-1200, Vector Labs). A Zeiss LSM710 confocal microscope was employed to perform slide examination and image acquisition. For immunohistochemistry analysis, sections were stained with the anti-von Willebrand factor antibody (vWF; 1:2000, ab6994, Abcam) followed by incubation with an HRP-conjugated anti-rabbit secondary antibody. Subsequently, specimens were incubated in diaminobenzidine (DAB), followed by haematoxylin counterstaining. vWF expression was quantified based on the measurements from three different randomly chosen fields (200×) in the implantation region. The images were acquired using a digital camera system (Nikon Coolpix). Semiquantitative evaluation of vWF expression was performed by using the integrated option density (IOD) score with Image Pro Plus 6 (Media Cybernetics).

Statistical Analysis

Statistical analysis was performed using a one-way ANOVA test. $*p < 0.05$ and $**p < 0.01$ were considered significant. All values are reported as a mean ± standard deviation.

Reference:

[1] H. J. Jeon, J. S. Kim, T. G. Kim, J. H. Kim, W.-R. Yu, J. H. Youk, *Appl. Surf. Sci.* **2008**, 254, 5886.

[2] M. J. Pereira, B. Ouyang, C. A. Sundback, N. Lang, I. Friehs, S. Mureli, I. Pomerantseva, J. McFadden, M. C. Mochel, O. Mwizerwa, P. Del Nido, D. Sarkar, P. T. Masiakos, R. Langer, L. S. Ferreira, J. M. Karp, *Adv. Mater.* **2013**, 25, 1209.

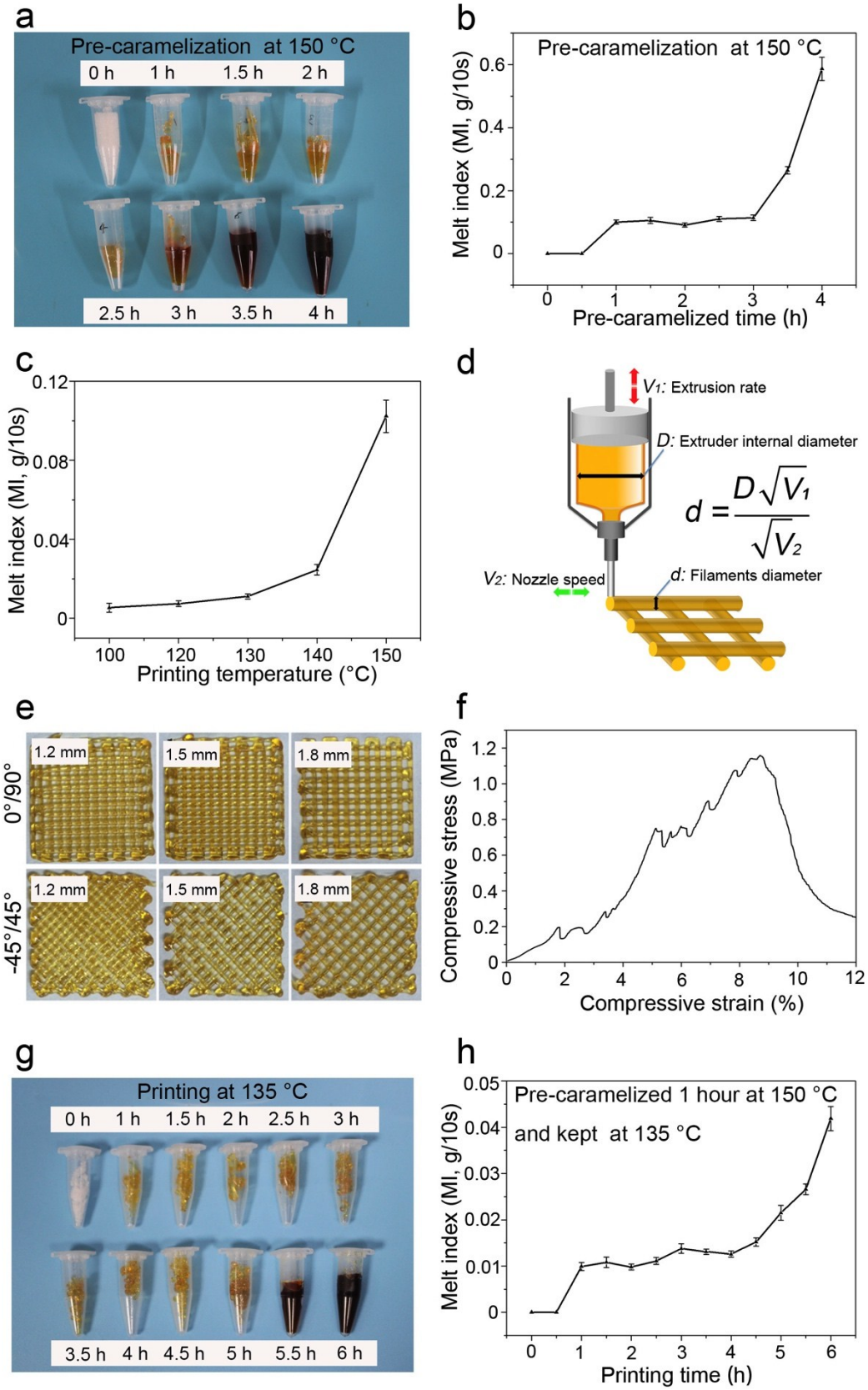

Fig. S1 The optimization of fabrication process, and characterization of caramel-based templates. (a) Photographs of a series of caramel produced from sucrose powder by heating at 150 °C indicated that 1-2.5 hours was suitable time to furnish caramelized sucrose for following 3D printing. (b) The melt index (MI) of caramelized products on different levels showed that the uncaramelized sucrose powders could not be heat extruded, the moderate caramelized products had stable thermal plasticity of extrusion, and the extrusion flowability of over-caramelized products became unstable and uncontrollable. (c) The MI of moderately

caramelized products at different printing temperature showed that the extrusion flowability was inversely aligned to temperature. When the temperature over 140 °C, the viscosity of the caramelized products were drastically reduced, leading to poor ability to maintain its printed prototype. Correspondingly, we choose 135 °C as the printing temperature. (d) Theoretical model of the relationship between filament diameters and extrusion rates while keeping other conditions consistent. (e) Templates with different spacings (1.2 mm, 1.5 mm, 1.8 mm) between filaments and lay-down patterns (0°/90° or -45°/45°) were printed. (f) Representative stress-strain curve of caramel-based template in uniaxial compression testing revealed that it was rigid with good ability to keep shape. Filaments were crushed one by one. (g) The sucrose pre-caramelized at 150 °C for 1 hour could be printed at 135 °C for additional 4 hours without significant appearance change. (h) The MI of moderately caramelized products could keep stable for at least three hours for controllable printing process.

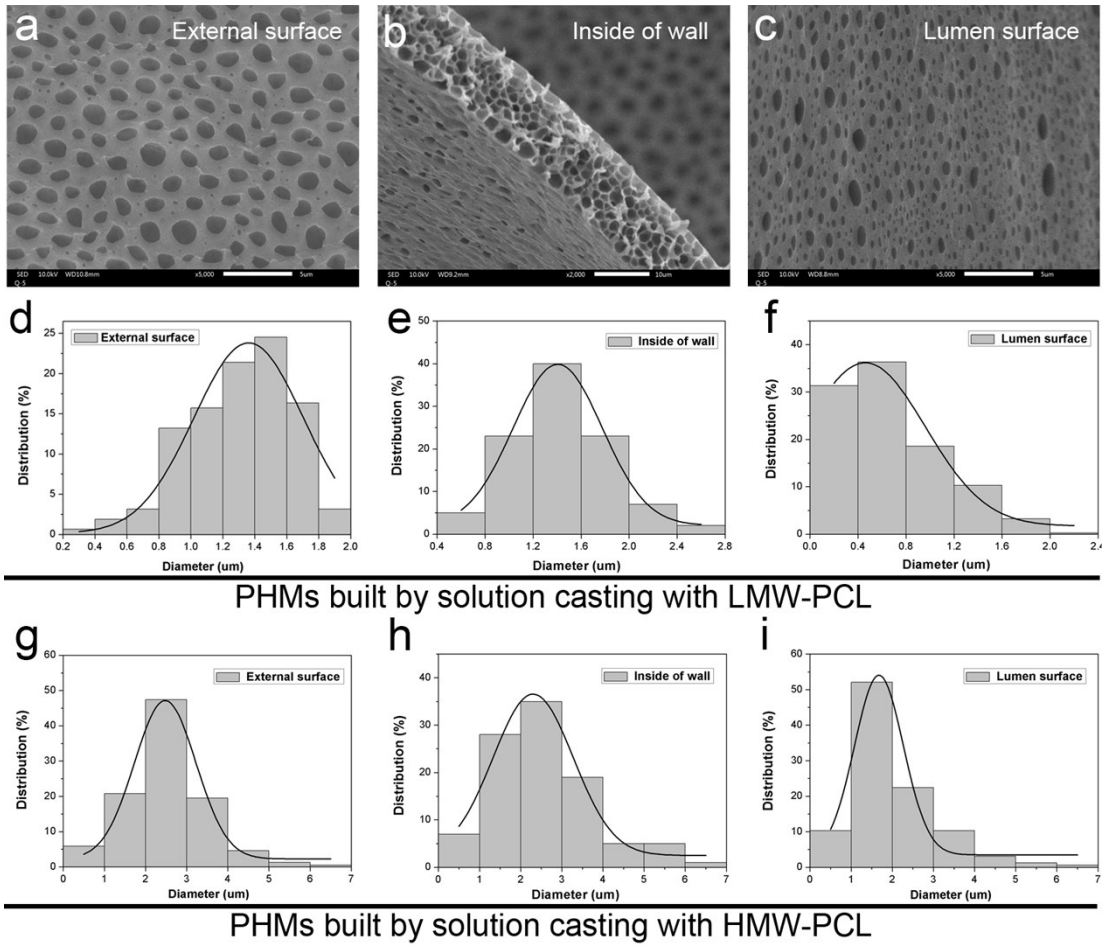

Fig. S2 The morphology of PHMs by PCL/HFIP solutions casting with different molecular weight. (a-c) SEMs of PHMs using LMW-PCL. Pores were uniformly distributed throughout the external surface (a), inside of channel walls (b), and lumen surface (c). (d-f) Distribution and the fitting normal curves of pore size on the external surface (diameter = 1.31 ± 0.34 μm), inside of channel walls (diameter = 0.68 ± 0.41 μm) and lumen surface(diameter = 1.42 ± 0.41 μm) by using LMW-PCL. (g-i) Distribution and the fitting normal curves of pore size on the external surface (diameter = 2.50 ± 0.98 μm), inside of channel walls (diameter = 1.98 ± 1.0 μm) and lumen surface(diameter = 2.57 ± 1.30 μm) by using HMW-PCL.

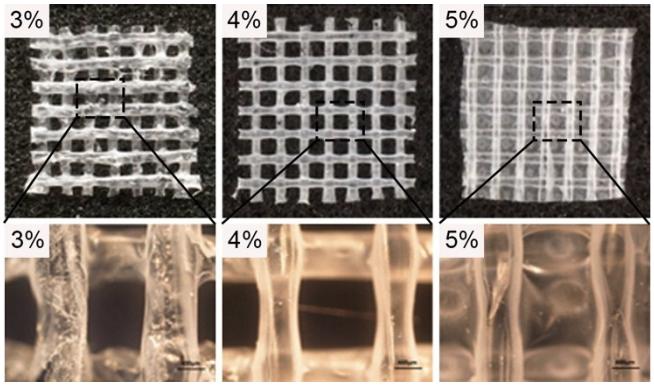

Fig. S3 The PHMs made from different concentrations of 3%, 4% and 5% (w/v) in HFIP solutions (HMW-PCL).

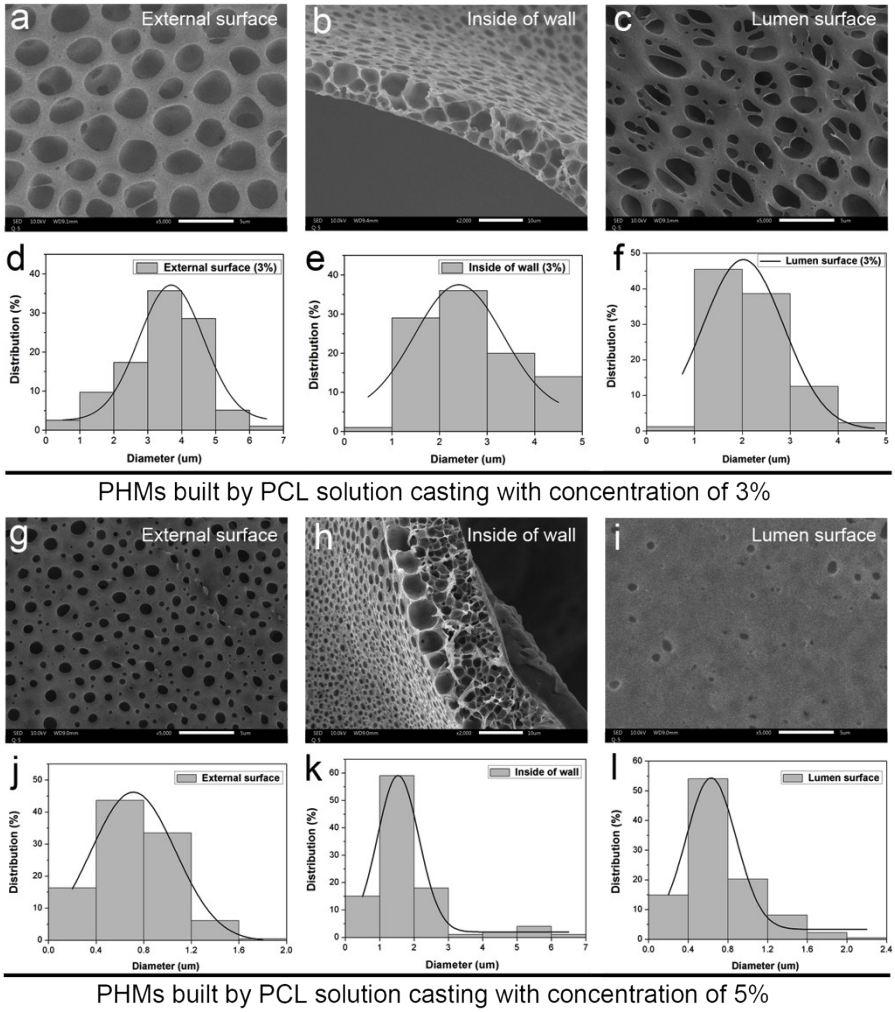

Fig. S4 The microstructures of HMW-PCL PHMs by HFIP solutions casting with different concentrations. (a-c) SEMs of PHMs made from polymer solution with concentration of 3% (w/v). The PHMs exhibited larger-scale pores and thinner wall. (d-f) Distribution and the fitting normal curves of pore size on the external surface (diameter = 3.47 ± 1.1 μm), inside of channel walls (diameter = 2.63 ± 1.02 μm) and lumen surface(diameter = 2.2 ± 0.82 μm). (g-i) SEMs of PHMs made from polymer solution with concentration of 5% (w/v). The PHMs exhibited smaller-scale pores and thicker wall. (j-l) Distribution and the fitting normal curves of pore size on the external surface (diameter = 0.73 ± 0.29 μm), inside of channel walls (diameter = 1.83 ± 1.08 μm) and lumen surface(diameter = 0.72± 0.36 μm)

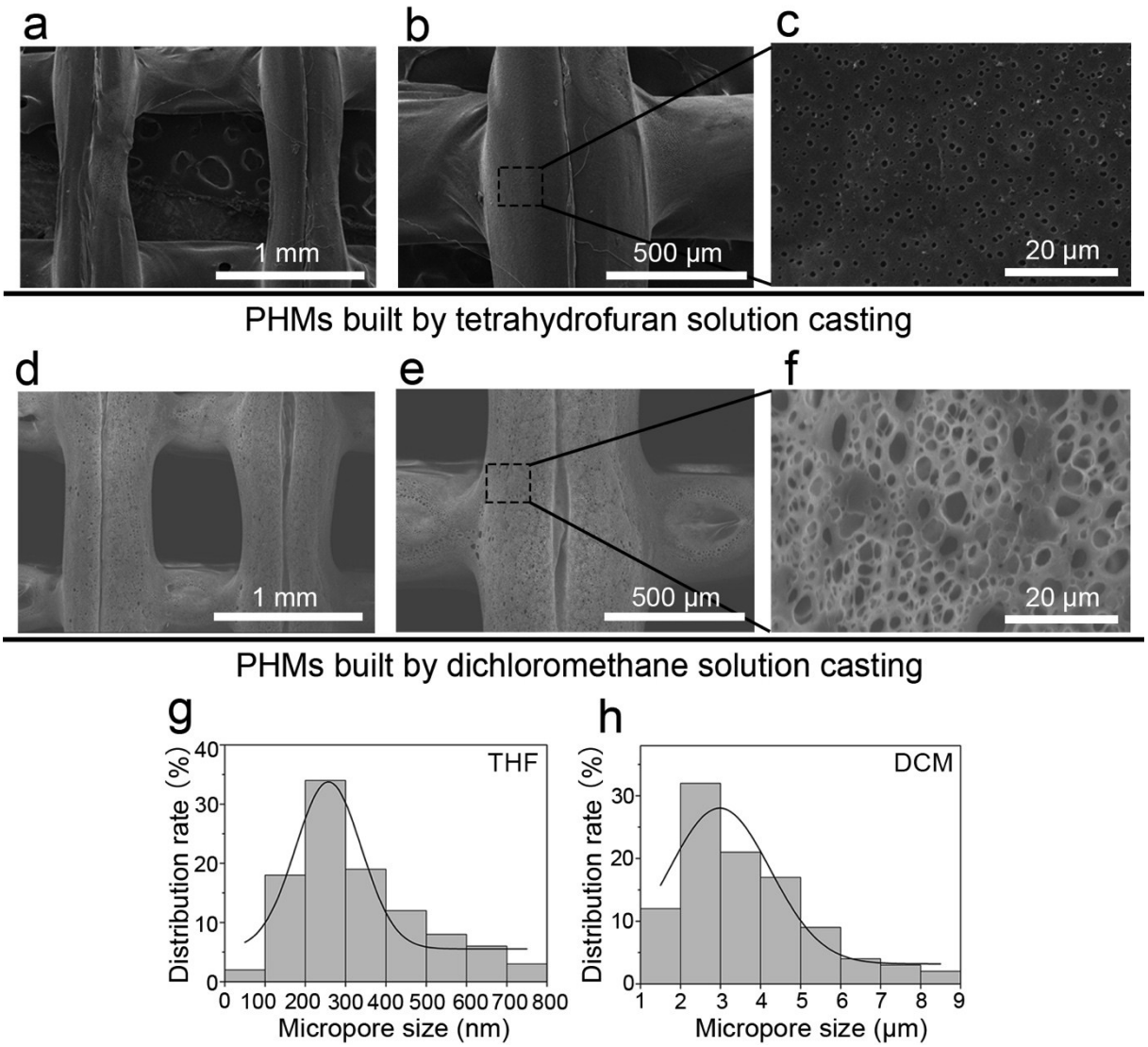

Fig. S5 The morphology of HMW-PCL PHMs made from different organic solvents with concentrations of 4%. (a-c) SEMs of PCL PHMs using THF as organic solvent. Pores were distributed on the external surface in the nanoscale. (d-f) SEMs of PCL PHMs using DCM as solvent. Pores were distributed on the external surface in the microscale. g,h) Distribution and the fitting normal curves of pore size on the external surface by using THF (g) and DCM (h).

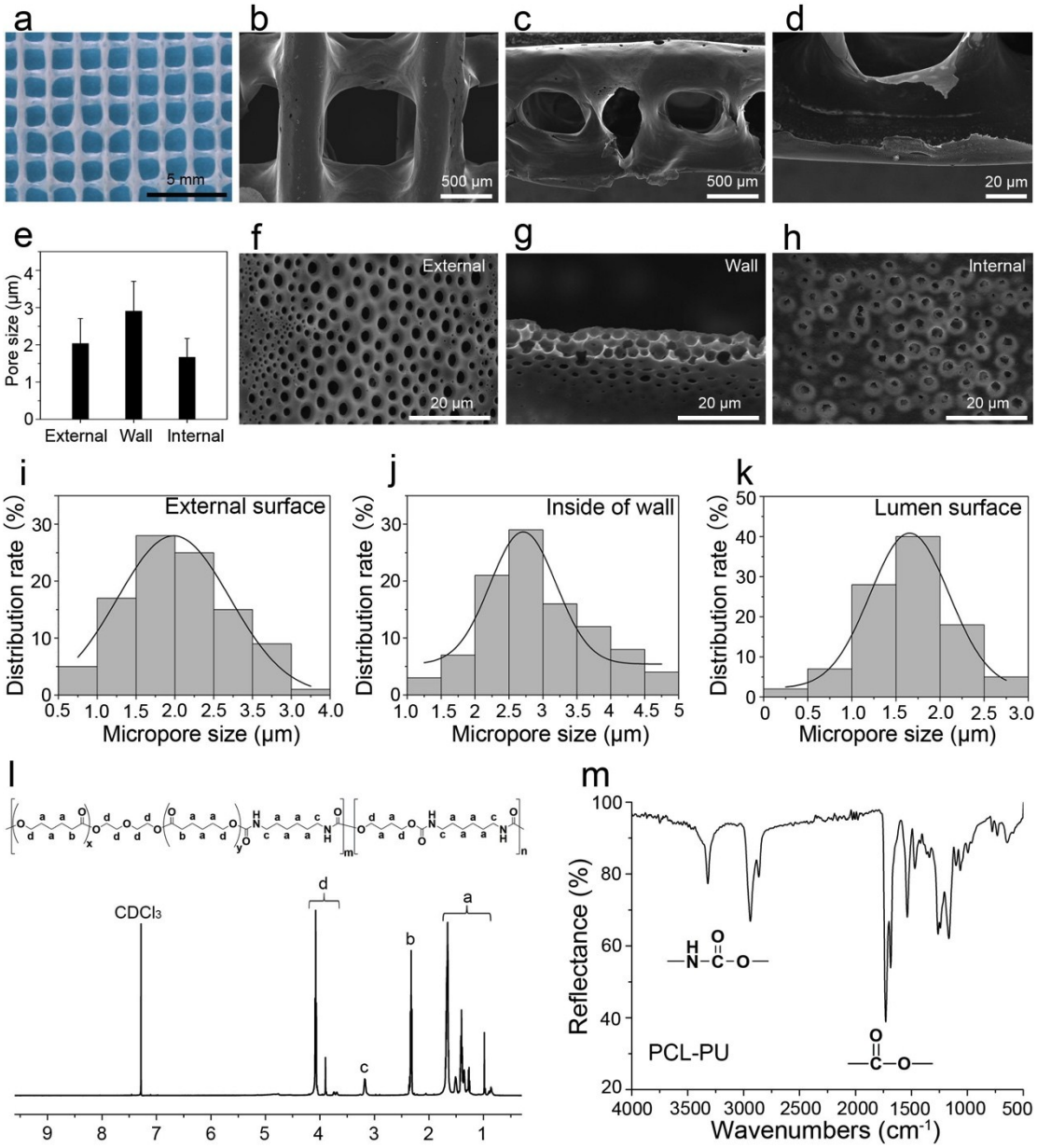

Fig. S6 Elastic PHMs made of representative thermoplastic PCL-PU bioelastomers. (a-h) Morphology of PCL-PU PHMs. Macroscopic optical image (a), microscopic SEM images in top view (b), side view (c) and lumen section (d), clearly showed PCL-PU PHMs had hierarchical structures with well aligned multilayer network built by interconnected channels. SEM images of magnified external surface (f), inside of channel walls (g) and lumen surface (h), and the corresponding quantitative analysis (e) of pore size confirmed the microporous structures in the walls of PCL-PU PHMs. (i-k) Distribution and the fitting normal curve of pore size of PCL-PU PHMs on the external surface (2.03 ± 0.67 μm, i), inside of channel walls (2.90 ± 0.80 μm, j) and lumen surface (1.67 ± 0.51 μm, k). (l) Molecular formula and nuclear magnetic resonance (^{1}H NMR) of PCL-PU elastomer. (m) Fourier transform infrared spectrum (FTIR) of PCL-PU PHMs.

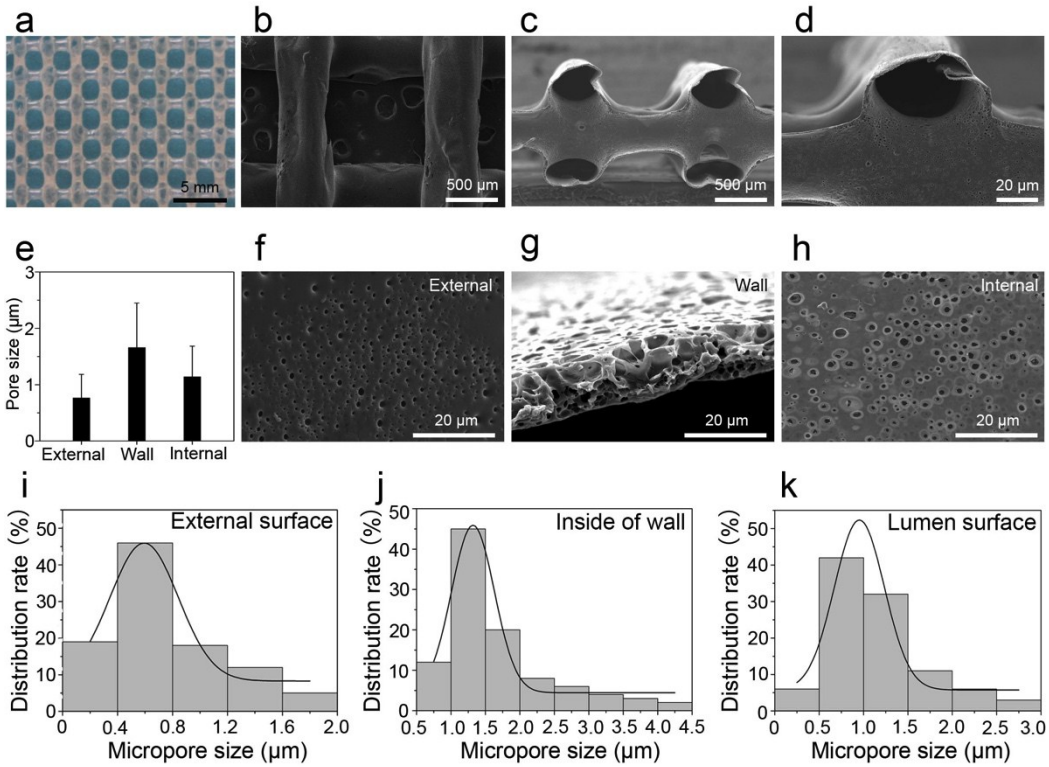

Fig. S7 Elastic PHMs made of representative thermoset PGSU bioelastomers. (a-h) Morphology of PGSU PHMs. Macroscopic optical image (a), microscopic SEM images in top view (b), side view (c) and channel section view (d), clearly showed PGSU PHMs also had hierarchical structures with interconnected channeled networks. SEM images of magnified external surface (f), inside of channel walls (g) and lumen surface (h), and the corresponding quantitative analysis of pore size revealed the microporous structures in the channel walls of PGSU PHMs (e). (i-k) Measurement and statistics, and the fitting normal distribution curve of pore size of PGS PHMs on the external surface (0.76 ± 0.42 µm, i), inside of channel walls (1.66 ± 0.79, µm j) and lumen surface (1.14 ± 0.54 µm, k).

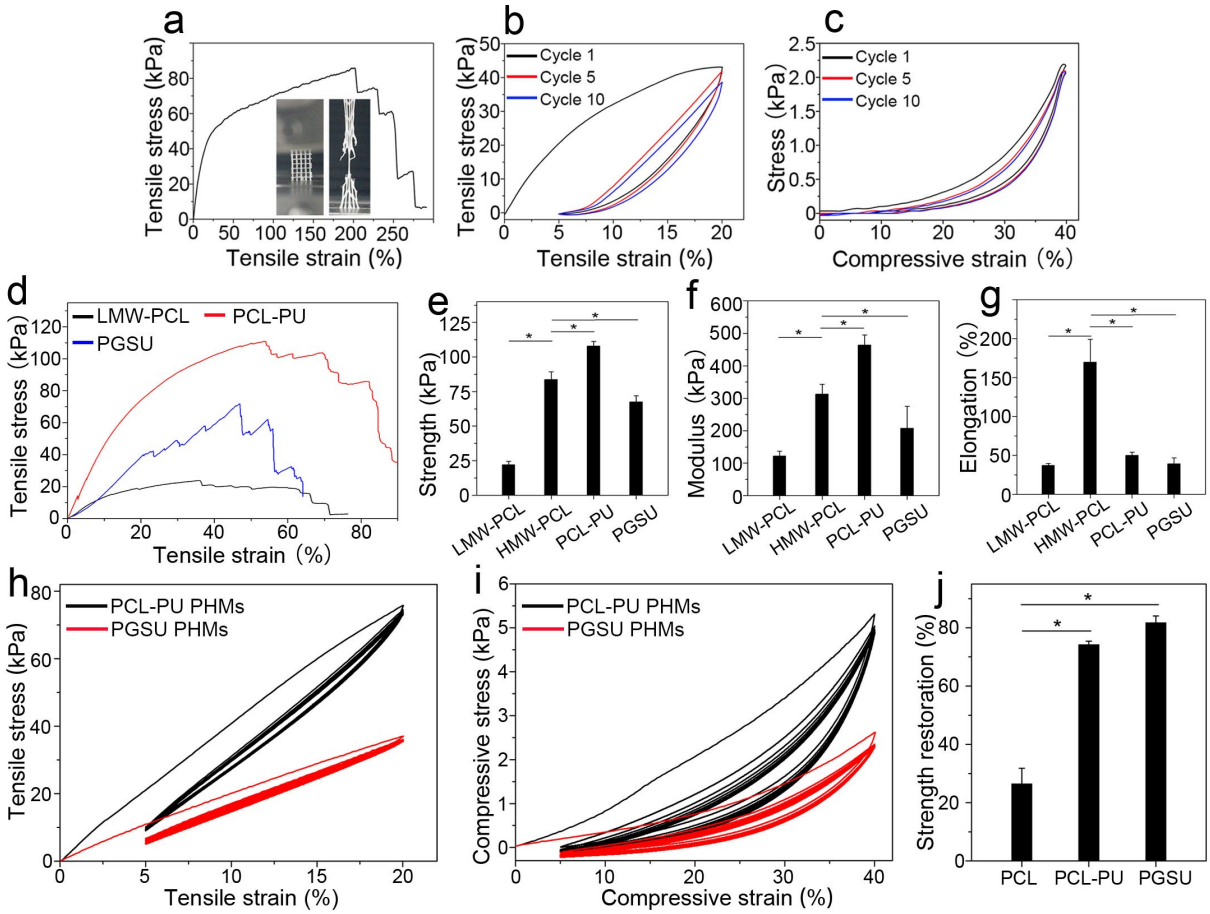

Fig. S8 Tunable mechanical properties of PHMs. (a-c) Mechanical properties of HMW-PHMs. Typical stress-strain curve of simple tensile test (a), cyclic tensile (b) and compression tests (c) for 10 cycles at a strain of 20% and 40%, respectively, revealed the anti-fatigue properties of PHMs. (d-j) Tunale mechanical properties of PHMs made from different materials. (d) Typical tensile stress-stain curves of LMW-PCL PHMs, PCL-PU PHMs and PGSU PHMs. Comparison of the tensile strength (e), Young's moduli (f) and elongation at break (g). Cyclic tensile (h) and compression tests (i) for 10 cycles at 20% and 40%. (j) The comparison of dynamic tensile strength restoration at a strain of 10% from 2nd to 10th cycles compared to 1st cycle of different PHMs.

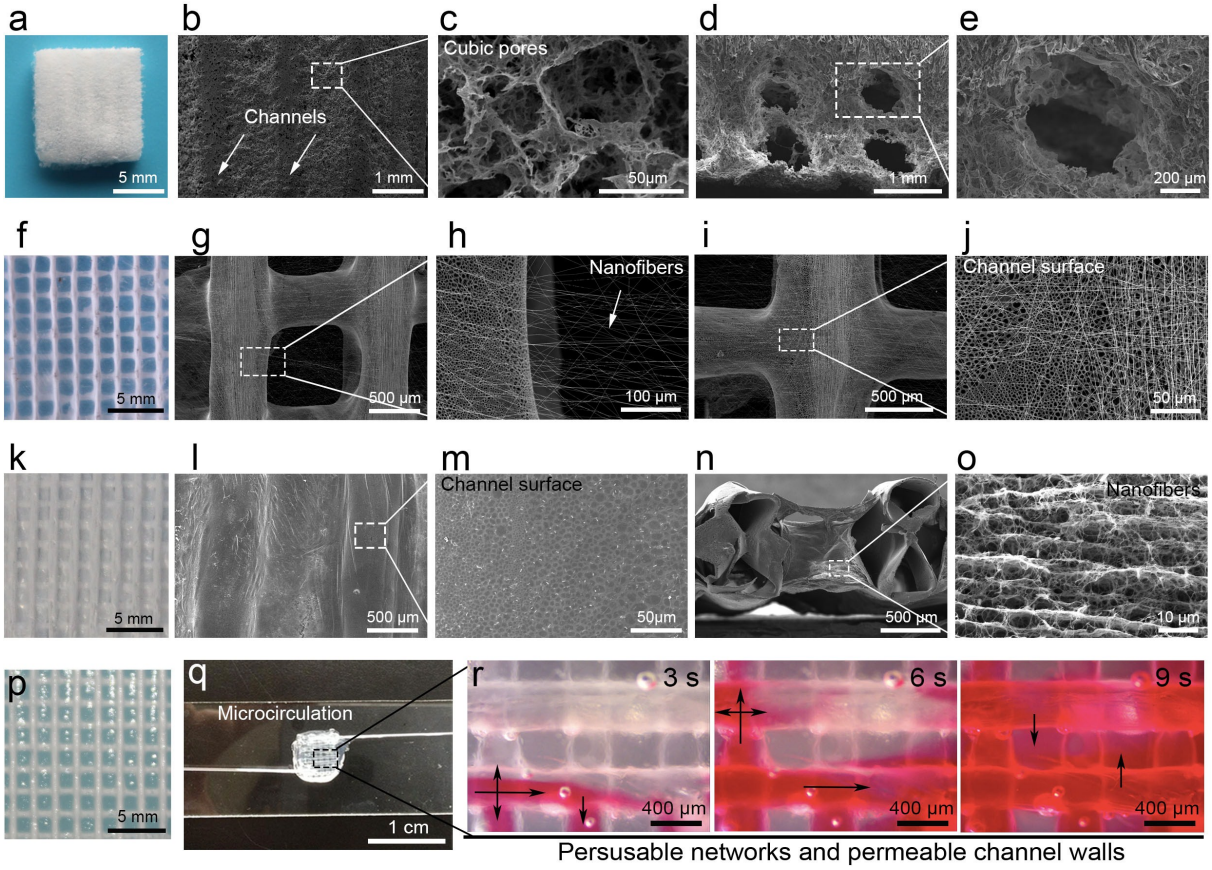

Fig. S9 Hierarchical composite scaffolds with built-in transport system. (a-e) 3D porous scaffold with build-in interconnected channeled network. (a) Macroscopic optic image. SEMs of top view showed build-in parallel channels (b) and porous structure (c) with porogen-genenerated cube-like pores and extensive micropores in the interstitial space between channels. SEMs images of cross-sectional view showed arrayed channels (d) were surrounded by micropores (e). (f-j) Composite PHMs surrounded by electrospun nanofibers. (f) Macroscopic optic image. SEMs of channeled network (g) and lapped junction (i) showed uniform distribution of electrospun nanofibers surrounding patterned channels (h) with porous surfaces (j). (k-o) Bacterial cellulose impregnated PHMs. Macroscopic optic image (k) and SEMs of top view (l) and cross-sectional view (n) revealed the good integration of porous channeled networks (m) and bacterial cellulose nanofibers (o) and. (p-r) Hydrogel encapsulated PHMs. Macroscopic optic images (p) of hydrogel encapsulated PHMs and its upgraded microvasculature device (q). Time-lapse optical micrographs (r) of the perfusion of red dye solution throughout the build-in vasculature networks with gradual diffusion to surrounding hydrogel matrix demonstrated the substantial mass transportation and exchange ability of PHMs.

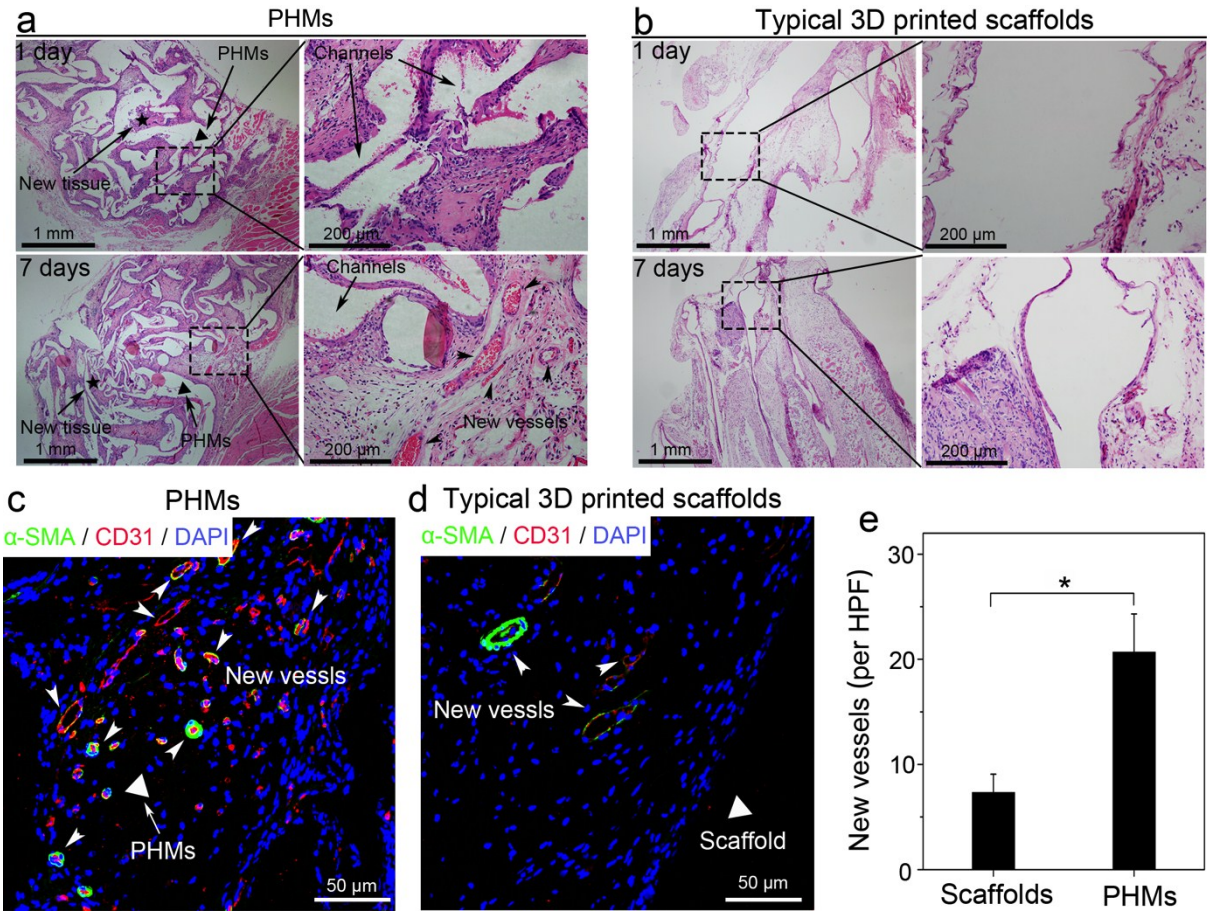

Fig. S10 Tissue growth and vascularization of PHMs and typical scaffolds in subcutaneous. H&E staining of PHMs (a) and control group (b) at predetermined time points (1, 7 days post-implantation). (c,d) Immunofluorescence staining of α-SMA (green), CD31 (red) and DAPI (blue) for new vessels and ingrowth tissue at 14 days post-implantation. (e) The quantification for α-SMA and CD31 positive vessels (average ± s.d., n = 9). *: Statistically significance, *$p < 0.05$.

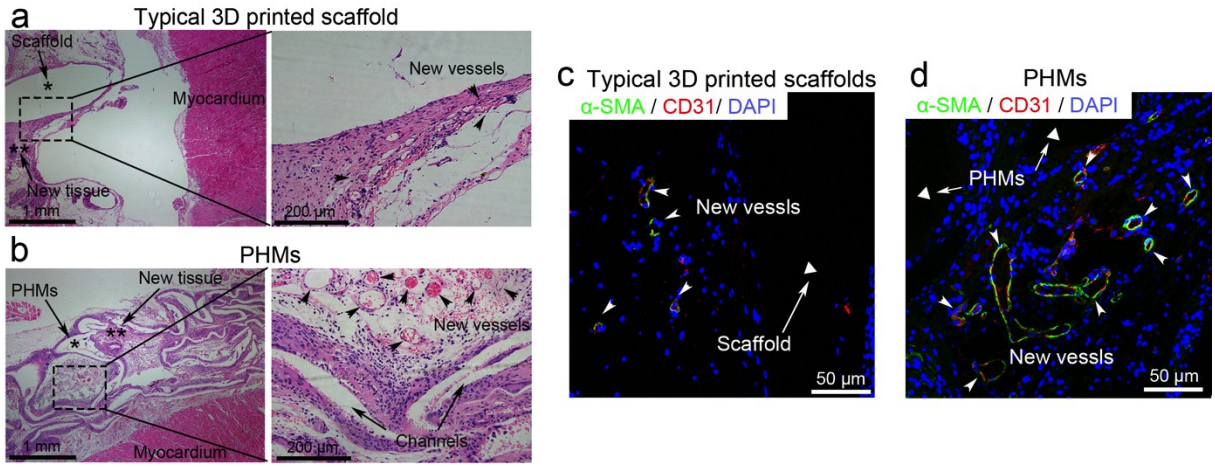

Fig. S11 Tissue growth and vascularization of PHMs and typical scaffolds in epicardial implantation. H&E staining of control group (a) and PHMs (b) at 14 days post-implantation. (c,d) Immunofluorescence staining of α-SMA (green), CD31 (red) and DAPI (blue) for new vessels.

Movie S1

This Movie shows the 3D priting process of caramel-based template. The caramelized sucrose was squeezed out by extrusion ram with a cylindrical nozzle temperature of 130 °C and rapidly deposited onto a stage. Multilayered caramel-based template (length × width = 20 × 20 mm) was fabricated in minutes with the accurate movements of extrusion system and x-y stage according to the theoretical model path. The center-to-center distance between filaments was 1.2 mm with 0°/90° lay-down patterns between two successive layers. The height of every layer was 0.5 mm. Being cooled in the air, filaments of adjacent layers combined together firmly and kept the uniform cylindrical morphology. This caramel-based caramel could keep appropriate printability for a few hours.

Movie S2

This Movie shows the the removal process of caramel-based template. Distilled water added from one side of the PCL polymer coated template readily dissolved caramel filaments and flowed through the whole network in minutes to provide pre-desgined PHMs.

Movie S3

This Movie shows the macroscopic process of the perfusion of PHMs at 8x speed display. PHMs was connected to a syringe pump to assemble a microfluidic device. The liquid dye pumped from the inlet readily perfused the whole PHM. There was no apparent leaking.

Movie S4

This Movie shows the microscopic process of the perfusion of PHMs.

Movie S5

This Movie shows tensile test of a PCL PHMs at 8x speed display. The PHMs well kept the structural integrity up to a strain of 150%.

Movie S6

This Movie shows perfusability and permeability of the hydrogel encapusaled PHMs composite scaffold. A red dye aqueous solution was introduced into PHMs via a syringe pump. The dye liquor ran through the built-in PHMs. The open micropores on channel wall served as penetrative architecture to support the gradual diffusion of liquid dye from channels into gel matrix. These results suggested the good mass transport capability of PHMs.